Chapter 6

Materials and Processes for Ion Permeable Separating Membranes by Electro-Spinning

Rocío del A. Cardona and Jorge J. Santiago-Avilés

Additional information is available at the end of the chapter

http://dx.doi.org/10.5772/57094

1. Introduction

This chapter describes the generation of polymeric and composite materials, and their pertinent processing sequence for the fabrication of ion permeable membranes utilized in super-capacitors and other bipolar charge storage devices. Energy storage devices are conspicuous and ubiquitous these days. Mostly, because we are utterly dependent on electric energy for so many facets of our life, from the trendy and somewhat common electric or hybrid car, to the more rare, but no less useful pacemaker that keeps the heart pumping periodically for those in need for such device. Electric energy is so useful, because its versatility. Electric energy can be used to activate actuators to generate forces or torque, to sense mechanical, thermal, optical and chemical variables, to generate radiation fields for wireless communications, and in many other tasks. The problem with electrical energy is that in contrast with the chemical energy stored in liquid fossil fuels such as gasoline, the amount of energy per unit volume or mass stored in batteries or capacitors is less than a tenth [1, 2] of that of gasoline. This low energy density means that large volumes and masses are required to store reasonable amounts of energy resulting in reduce range for electric vehicles and short intervals between charging for "smart" phones.

2. Batteries and super-capacitors

The desire to increase the energy density of electrical cells or batteries (collection of cells) is what drives research in electrical energy storage systems. From the $Zn/ZnCl_2$ Leclanché cell to the modern Li-ion or Li-polymer batteries, what the scientist and engineers have been seeking are larger capacities (Coulombs, or Ampere-Hours delivered) [3]. All batteries consist of two

electrodes, a salt-bridge (permeable membrane that allows for the transport of ions), and electrically conductive liquid called the electrolyte. Batteries are very low impedance current sources, meaning that they have a small series resistance, this series resistance is kept small by design in order to reduce the time it takes to discharge the battery or charge the battery in the case of rechargeables [3]. Multiple challenges remain, such as better electrode materials (the density of Li ions "stored" in an electrode can be enhanced by intercalation, a phenomenon occurring in layered materials such as graphite, where the ions penetrate between the material layers), better electrolytes, the use of environmentally friendly materials (such as substituting Li for Mg as the active ion), and the use of inexpensive materials. Although electrical storage systems, such as batteries, are incapable of storing as much energy as liquid fossil fuels, for portable room temperature operations they avoid the burden that fossil fuels imposed as one try to extract the energy content stored in the chemical bonds, which require their oxidation or "burning" at high temperatures. Is evident that for this to happen at room temperature the combustion process must be thermally isolated, not a particularly inexpensive proposition, so under these circumstances batteries are a very good option.

Batteries are not the only charge storage device currently utilized or being researched. A relatively new breed of capacitors, called electrochemical capacitors, or depending on its formulation and operation, also called super-capacitors or pseudo-capacitors are been explored as potential energy storage devices [4]. The difference between these and the usual capacitors utilized in electronics / electrical applications is the capacitance or amount of charge stored per volt. The definition of a capacitor is therefore,

$$C = \frac{Q}{V} \tag{1}$$

Where C is the capacitance value, Q the stored charge in Coulombs, and V the electric potential in Volts. In terms of materials parameters and dimensions, another simple version of this relation is given by:

$$C = \frac{kA}{d} \tag{2}$$

In this case k is a material parameter, namely the product of ε the relative permittivity, and ε_0, the permittivity of free space, A, the effective capacitor area and d, the distance between the positive and negative charges. This last relation is fundamental in the understanding of these electrochemical super-capacitors functioning, as it is described in page 3 of this chapter.

3. Electrical double layer and pseudo-capacitors

There are two distinct types of electrochemical super-capacitors with different phenomena utilized as a charge storage mechanism. The first type is called an electrical double layer (EDL)

http://dx.doi.org/10.5772/57094

super-capacitor, and the second is called a redox pseudo-capacitor [4]. The first type, store charges utilizing the physical phenomenon of a double layer, where in the first layer lies negative charges (electrons) placed in the electrodes by a voltage bias, and the second layer is formed by mobile ions in an electrolyte. An EDL is formed when you immerse a conductor in an electrolyte, and proceed to bias the conductor. In that case, electrons are injected into the conductor, producing an attractive electric field to the positive ions in the electrolyte. These ions move to the surface of the conductor in order to minimize the distance between opposite polarity charges, forming the so-called inner Helmholtz layer. Since one can place more electrons in the conductor than there are ions in the electrolyte, not all the electric field from the conductor is cancelled, and more ions are accommodated increasingly farther away from the surface and the inner Helmholtz layer, forming the outer Helmholtz layer and the diffuse layer. The average distance from the conductor, where the diffuse layer ends, is called the Debye Length. See figure 1 for a schematic of the EDL.

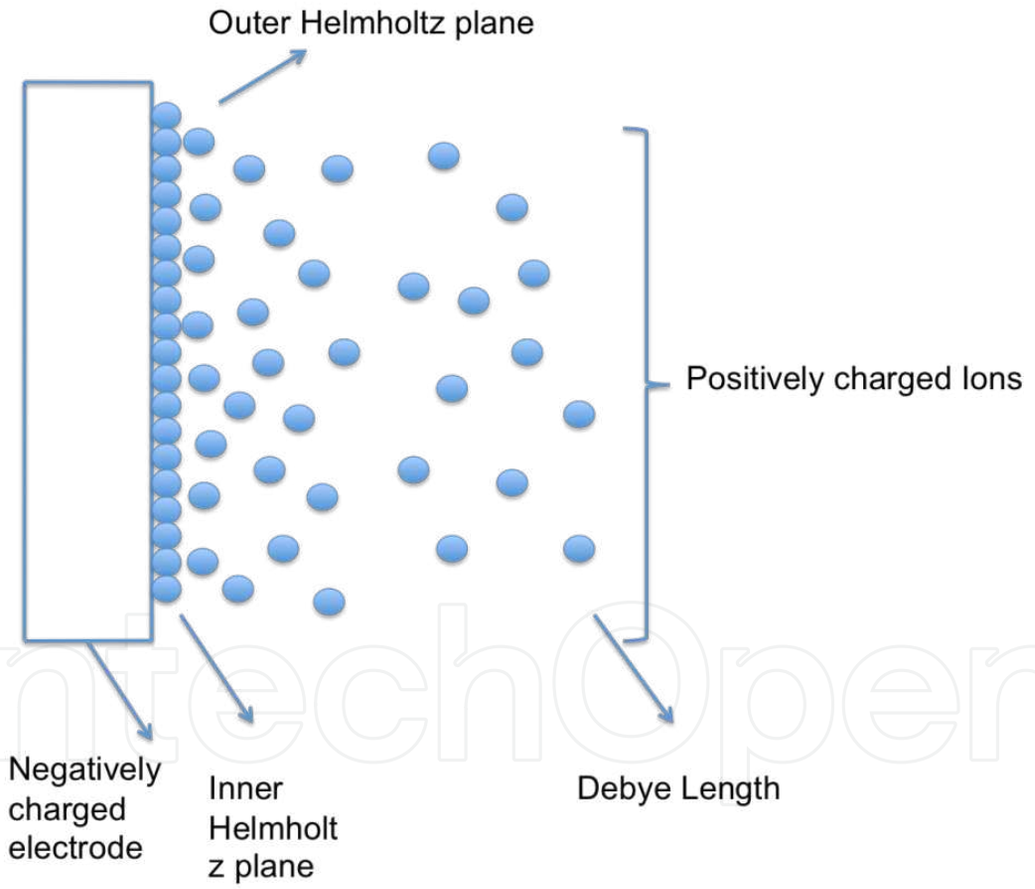

Figure 1. Simplified graphical description of the Electrical Double Layer (EDL).

For the second type, one has one or two electro active polymers (EAP) electro-deposited onto a metallic current collector and bathed by a suitable electrolyte. When you place opposite polarity voltage bias in the two electrodes, the built-on electric field attracts ions from the electrolyte, which undergo redox reactions placing charges in the peripheral chemical groups

of the EAP. If you find that this second type looks a lot like a battery, you are completely correct, it is a battery that can be charged and discharged quickly and for the electric circuit, if it behaves as a capacitor, it must be a capacitor. Since the phenomena mediating in the charge storage for this type of capacitor is chemical, they are generally addressed as pseudo-capacitors. From equation 2, one may note that capacitance increases with the effective area, which in the case of a DLC device, the area can be enhanced by using a high specific surface area (SSA) conductor such as activated carbon or any of a multiplicity of carbon allotropes [5] such as Graphene, carbon nano-tubes, carbide derived carbons, carbon onions and perhaps others.

4. Materials and models

Some of these materials possess SSA as large as 3,000 m^2 /g. The other geometrical parameter in equation 2 is d, the separation between oppositely charged particles, in this case, electrons in the electrode and ions in the electrolyte. As electrostatics demands, the mobile ions will lie on the surface of the carbon electrode pores, making d of nanoscopic dimensions. This combination of large numerator and small denominator leads to a large value of the capacitance, as large as several hundred Farads [4]. Super-capacitor in general consists of two capacitors in series, the one electrode biased negatively will attract the positive ions and the other, biased positively, will attract the counter-ions. For this reason, relation 3 gives the total capacitance, namely:

$$\frac{1}{C_T} = \frac{1}{C_1} + \frac{1}{C_2} \tag{3}$$

Note that some electrolytes are of the aqueous type (a salt dissociated in water) and other use more sophisticated organic liquids or ionic liquids, these last two, organic in origin and capable of sustaining larger voltages before degrading [4] as implied in the following relation (equation 4):

$$E = \frac{1}{2} CV^2 \tag{4}$$

Where, E is energy in Joules, C capacitance in Farads and V electrical potential in volts. Both types of super-capacitors have the distinct characteristic that they can be charged and discharged very quickly (the DLC more than the redox). Since you are doing work in order to load energy into these devices, and how quickly you do work (or use energy) is power, these super-capacitors possess large power densities (power per unit weight, or gravimetric power density, or power per unit volume, or volumetric power density). Most super-capacitors share a common configuration. If we look at one of those devices edgewise, they possess the packaging (usually metallic or polymeric), a metallization as a current collector for one of the electrodes, the electrode material (usually a carbon allotrope or a EAP / composite), the

http://dx.doi.org/10.5772/57094

electrolyte, and the separating membrane. The structure is symmetric, so the other side is pretty much the same sequence in reverse order. Figure 2 shows a schematic of a super-capacitor configuration and the inner details of its working. The simplest way of modeling a super-capacitor is by an ideal capacitor with a resistor in series. This resistor is a lump parameter, and includes all possible phenomena offering resistance (or impedance) to the flow of current, including the electrolyte, the electrodes, the current collectors, the external contacts, etc. One key aspect in the construction and improvement of EDLC is the ion permeable separator that prevents electrical contact between the conducting electrodes (shorting), but still allows ions from the electrolyte to pass through. Most of the membranes currently used, are made from polypropylene [6], a thermoplastic polymer that among other characteristics, can stand the chemical environment to which they are exposed. However, its use is limited due to UV-Vis degradation and low biocompatibility.

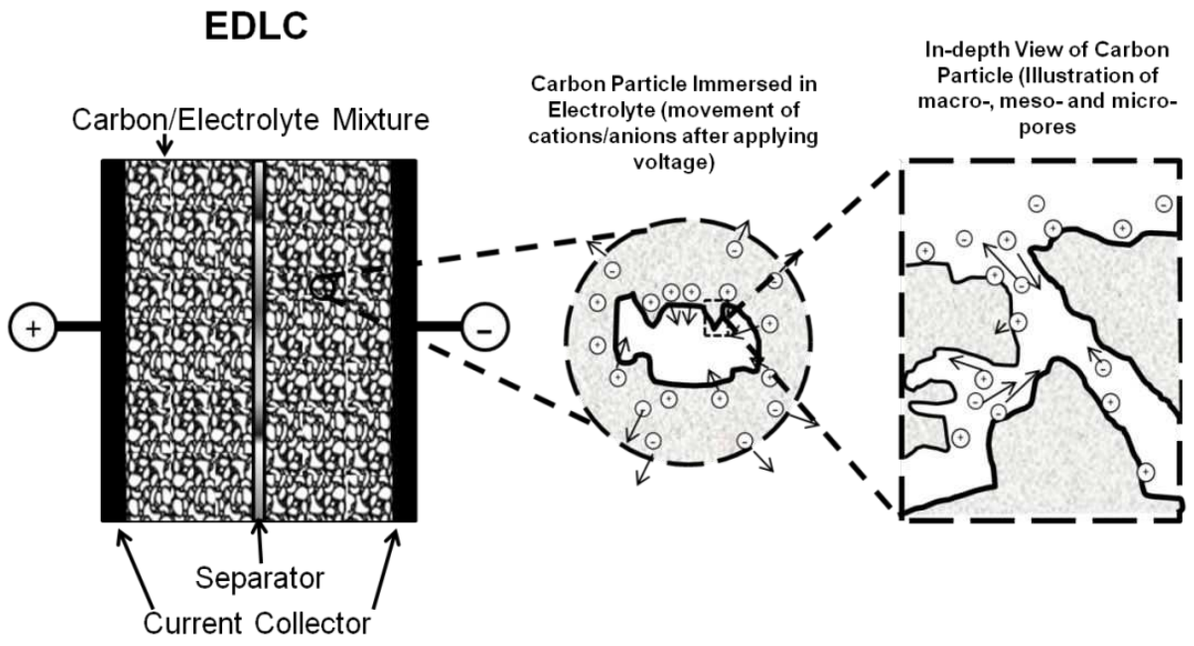

Figure 2. Schematic of the super-capacitor configuration and inner working details (not to scale).

5. Separating membranes

Ideally a good separating membrane will be thin (10-15 μm), mechanically strong (1-4 GPa), chemically inert to the electrolyte utilized, electrically insulating ($R>10^8$ Ω), and thermally stable. The high resistivity of the composite membrane might be counter intuitive, as the filler are highly conductive carbon nano-tubes (CNT's). Remember that in order for the composite to conduct an electric current effectively (with low resistance), the CNT's must be touching each other making a conductive path from one electrode to the other, in a process called percolation. The amount of CNT's as filler added to a given amount of binder in the composite

as to provoke this change in resistance is called the percolation threshold (PT). Although the PT for most polymers is small, for PLA at the highest concentration used in this study, the membrane resistance exceeded tens of MegOhms.

Besides polypropylene another common separating membrane is a composite layer of poly-tetra-fluoro-ethylene (PTFE or Teflon) between nylon or polyester layers. Polypropylene is a low-density linear polymer often used for its reasonable mechanical properties and low cost. The PTFE composite (GoreTex™) [7] relies on the properties of PTFE whose mechanical properties are defined by the rate of the strain applied during its manufacture. If high enough, it produces billions of slit shaped nanoscopic pores per square inch, allowing the flow of ions but impeding the passage of particles or colloids. The polypropylene membranes are often weaved mechanically, but they can be electro-statically deposited by electro-spinning, a process that will be described shortly. Polypropylene is also notorious for its sensitivity to sunlight, in particular the UV part of the solar spectrum as mentioned above, where carbon bonds in their chain structures are attacked by the UV photons. The ultra-violet rays modify the affected bonds to form highly reactive free radicals, which then further react with atmospheric oxygen forming carbonyl groups in the main chain. These chemical transformations modify the polymer properties, in particular mechanical properties. The device might lose color and surface cracks will appear often leading to device failure. There are other types of membranes being explored for the particular application of electrochemical super-capacitors. Some work on bipolar membranes constructed using ion-exchange membranes (anions) and a cation exchange solution to form the bipolar structure. This proto-membrane is then coated with a NAFION layer. NAFION has been utilized using other formulations [8]. Sulfonated poly (ether ether ketone, SPEEK) has been used, as a proton conducting polymer membrane in similar applications [9].

6. Polylactic acid

In our laboratory we have been exploring materials for ion permeable separating membranes showing ease of fabrication (primarily electro-spinning), chemical and mechanical stability, and low cost.

Poly lactic acid, an alpha polyester discovered in 1932 by Carothers in DuPont [10] has been the polymer of choice. There are two main routes for the synthesis of PLA, direct condensation of lactic acid, which produce low molecular weight polymers (2,000-10,000). This procedure can be followed by de-polymerization to form a cyclic dimmer intermediate followed by a ring opening polymerization to produce high molecular weight PLA (>100,000). The process is solvent free which represent a synthetic advantages for the scaling up, minimizing waste disposal. An alternative approach to obtain high molecular weight PLA is using chain coupling agents or azeotropic dehydrative condensation (figure 3) [11].

One of the principal advantages of PLA is that the precursor monomer, lactic acid, can be obtained from renewable sources including the fermentation of molasses, potato starch, or of the dextrose from corn. It can also obtained from petrochemical sources, however, due to the

http://dx.doi.org/10.5772/57094

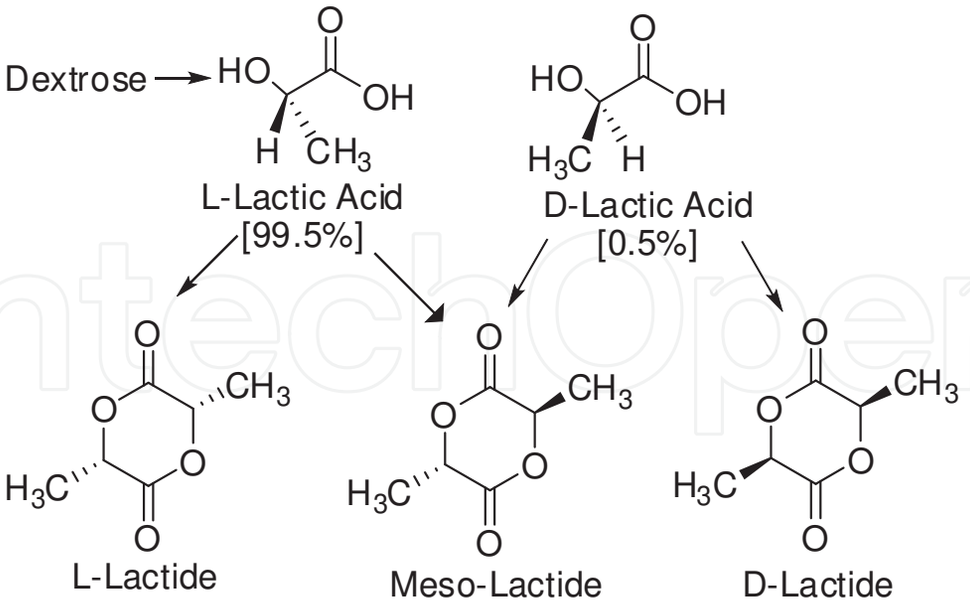

Figure 3. Synthetic routes for the production of Poly lactic acid

optimization of cornstarch bacterial fermentation using a Lactobacillus strain, this is now a days the most often employed method to obtained the monomer. Poly-L-lactic acid (PLLA), the principal product of the reaction under controlled synthetic conditions, is chiral, that is, it rotates the polarization plane of light, that is why the L, for levo-rotation. PLLA has a crystallinity of around 37%, a glass transition temperature between 60-65 °C, a melting temperature between 173-178 °C and a tensile modulus between 2.7-16 GPa. Interestingly, heat resistant PLLA can withstand temperatures of 110 °C (230F) [12]. These relatively high temperatures represent an adequate factor of safety for automotive and other traction applications of supercapacitors.

Besides its synthetic and physical properties advantages, PLLA is a biodegradable and biocompatible polymer approved by the FDA for food packaging and implantable medical devices, allowing it use in EDL applications as for example pacemakers.

There are several examples in the literature of PLA and other polymers [13] been combined with other materials to form composites. In a composite, one mixes (or react) two or more materials (phases) with diverse properties, to combine the effect of those properties in the product material or phase. In our continual study of materials for permeable membranes, we have combined the ease of fabrication by electro-spinning fibers formation of polymeric materials, with the enhanced mechanical and electrical properties of carbonaceous allotropes materials, and some metallic colloids such as silver. Although diamond and graphite are the most commonly mentioned allotropic phases of carbon, there are multiple members in this family, from graphene through various types of carbon nano-tubes and bucky-balls, to carbon onions, they span a gamma of physical and chemical characteristics of substantial relevance to super / pseudo- capacitor technology [14]. More on polymer based composites will be presented latter in the chapter.

7. Electro-spinning of polymers

Electro-spinning or electrostatic deposition is one of the easiest and most inexpensive methods of generating nanoscopic polymer / composite fibers of macroscopic lengths. In other words, the ease of processing, the low learning curve and inexpensive instrumentation render this technique extremely popular and versatile. One electro-spin viscous liquids, so having the right resin / solvent ratio, or in the case of composites, the right filler / binder / solvent proportions (and perhaps access to a good rheometer in order to characterize the polymer solution) is of some importance.

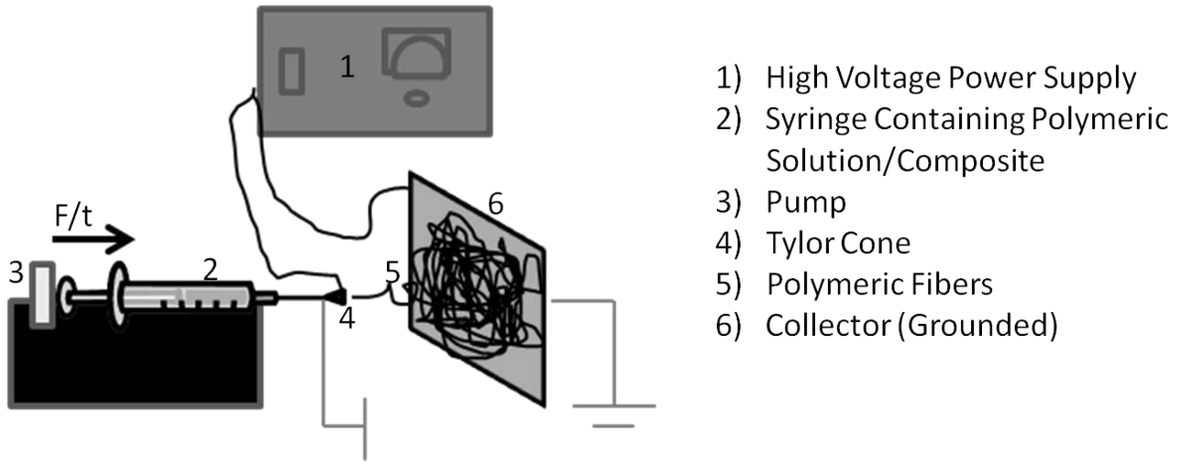

Figure 4. Details of a simple "home brew" electro-spinning apparatus.

The "home brew" configuration utilized in electro-spinning usually consists of a small (low power), high voltage power supply capable of voltage outputs in the range to several tens of kilovolts at very low current levels (below μA is desirable, see figure 4). A syringe pump, (to controlled the rate of fluid outcome from the syringe), syringe (containing the polymer solution), and an electrically grounded collector, complete the "home brew" set-up as shown above.

The morphology of the out coming fibers or mats will depend of several experimental conditions including: viscosity of the solution, applied electric field (applied voltage/needle to collector distance), the pump rate, temperature and pressure, solvent vapor pressure (evaporation rate), and collection time. Another method employed to control the fibers morphology (alignment) during electro-spinning is using a rotating collector or an oscillating needle [15]. These make electro-spinning a good tool to produce mats with a better-controlled morphology. A common morphological feature in electro-statically deposited fiber and mats is the formation of beads or beading. This particular feature involve the formation of random beads, preferentially where fibers cross each other, often due to the visco-elastic nature of the electro-spinned

http://dx.doi.org/10.5772/57094

precursor fluids or fluctuations in the deposition parameters. The mats permeability is a function of the pores dimensions distribution. These dimensions are statistically distributed and they tend to correlate inversely with the mat thickness or electro-spinning deposition time. The dimensions of most pores for reasonable deposition times (a few hours or less) lie in the range between micro and nano-meters, as evidenced by SEM micrographs.

8. Composites and characterization

In our studies, solutions of PLLA and PLLA- multi walled carbon nano-tubes (MWCNTS) composites were used. It is know that the addition of carbon nano-tubes to a polymeric solution can improved the mechanical properties of the resulting fibers and/or mat [16]. The PLLA was dissolved in 1:3 acetone/chloroform to prepare solutions of 13, 15 and 17 % w/v concentrations. The viscosity of the solutions were measured in a Bolin Rheometer with the following results, namely (1.1 +/_ 0.1, 2.8 +/_ 0.4 and 3.2 +/_0.6) Pa.s, respectively. As expected, viscosity increased as the content of polymer in solution is increased. These initial solutions were spun using the standard electro-spinning set-up, where the resulting fibers were collected in silicon wafers for subsequent structural analysis. The applied electric field during deposition was 2.3 kV/ cm, with a collection time of 10 s and a pump rate of 0.5 mL/hr. Usually for large anode-cathode distance, in excess of let's say 5 cm and a homogeneous solution, fibers diameters are randomly distributed usually following a log-normal distribution.

One problem when working with very small fibers, with diameters comparable to the wavelength of the visible light, is you inability to see or clearly image structural details such as diameters, asperities, and general morphological features. It is in such cases that scanning electron microscopy (SEM) can be a formidable characterization tool. Even when one ignores the differences in magnification between optical and SEM instruments (500,000 x, that is 250 times better magnification than a good optical microscope), the depth of field is what makes SEM such a versatile instrument. In optical microscopy, you can see the top of a micrometric diameter fiber, but not its sides or bottom, unless you move the focus. In SEM one sees around the complete fiber in focus, that is the top, sides and bottom. Of course, SEM requires a vacuum for the electron optics, and liquid samples, or samples involving liquids present serious imaging challenges. In our experimental work, SEM has been the instrument of choice for imaging and measure.

Analysis of SEM data for the fiber diameter reveals that as the solution viscosity increased, the diameter of the obtained fibers was smaller. One can see the effect by examining the distribution with a higher mean value of the fiber diameter (4 μm) for the 13 % w/v solution, and compare it to those with smaller mean diameters, i.e. (1 μm), for the 17 % w/v solution. Figure 5, show the SEM images of deposited fibers from different solutions and a histogram with the diameters frequency.

These experimental results on fibers diameter distribution suggested continuing further experimentation using the 15 % w/v solution. This particular solution produced fiber with an average diameter of (2.2±0.5) μm. It also, have no beading and more uniform morphology than

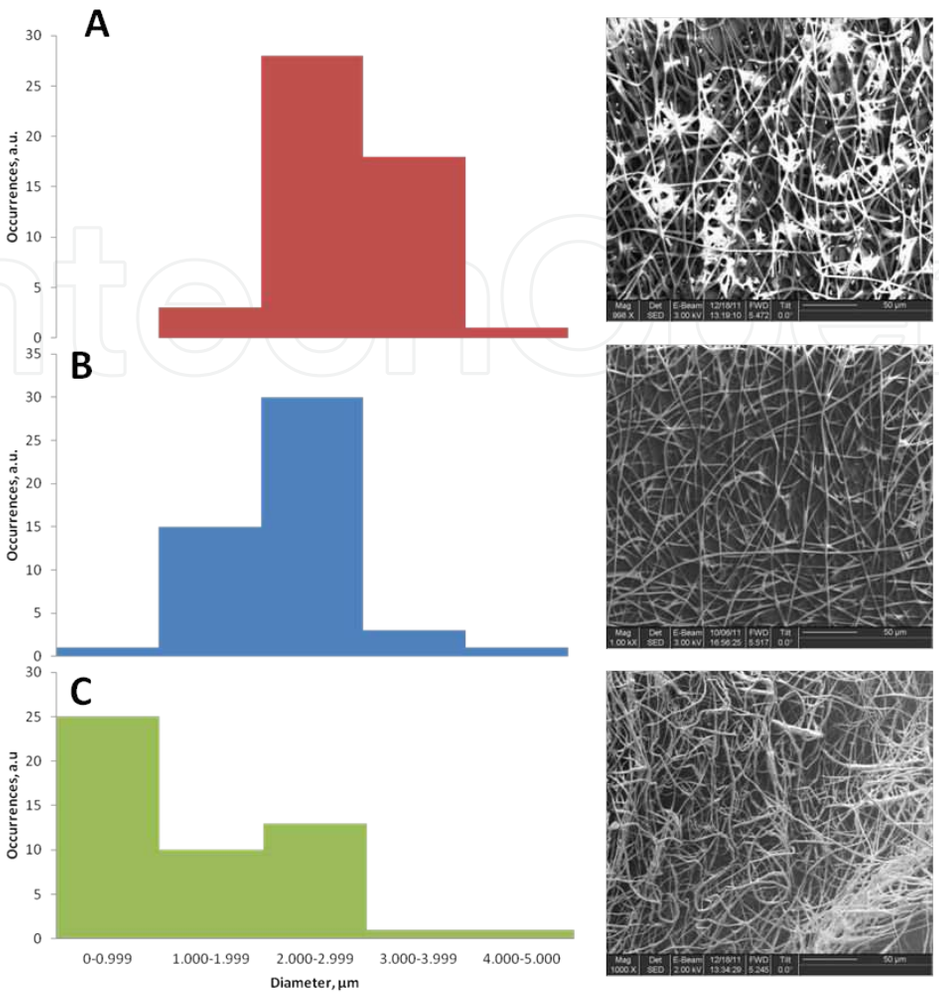

Figure 5. SEM images and data analysis for sample A) 13 % w/v PLLA, B) 15 % w/v PLLA, and C) 17 % w/v PLLA. All in 1:3 acetone/chloroform

the fibers collected from the other two solutions. These sets of facts are important, as later on they can be helpful in controlling the membranes morphology. As we proceed further, (0.2 mg/mL and 1.0 mg/mL) utilizing multi-walled carbon nano-tubes of different sizes, small (s), or large (l) (s-MWCNTs, 30-50 nm diameter, 0.5-2 μm length, and l-MWCNTs 60-100 nm diameter, 5-15 μm length), were added to the solution (15 % w/v PLLA). The viscosity of these solutions is lower than that of the pure PLLA solutions as expected, since the CNT's can only chemically interact through atoms lying in the prismatic planes (both ends of the tube) and defects, not through atoms in cylinder surface (the non-bonding π bands). Table 1 shows the viscosity data for all the solutions studied.

Figure 6 shows the SEM images and histograms for fiber diameter size distribution of 15 % w/v PLLA/ MWCNTs composites. From the SEM images we can observe that even when the viscosities of these solutions are similar, the morphology of the obtained fibers is affected by the size of the carbon nano-tubes.

http://dx.doi.org/10.5772/57094

Viscosity, Pa.s						
13%w/v PLLA	15% w/v PLLA	17% w/v PLLA	15% w/v PLLA (0.2 mg/mL s-MWCNT)	15% w/v PLLA (0.2 mg/mL l-MWCNT)	15% w/v PLLA (1.0 mg/mL s-MWCNT	15% w/v PLLA (1.0 mg/mL l-MWCNT
1.1 ± 0.1	2.8 ± 0.4	3.2 ± 0.6	1.6 ± 0.2	1.3 ± 0.1	1.5 ± 0.3	2.1 ± 0.6

Table 1. Viscosity as a function of composition for PLLA / MWCNT composites.

Note, how the diameters distribution shift to nano-metric size fibers for the solutions containing s-MWCNTs (figure 6, a-b) in comparison to the solutions containing l-MWCNTs (figure 6, c-d). From SEM images it can also be observed that the addition of l-MWCNTs seems to promote the formation of beads within the fibers. In order to study the suitability of PLLA/ MWCNTs composites in the production of membranes, the electro-spinning set-up was modified, using as a collector a rotating cylinder. The electro-spinning conditions were kept as before (applied electric field was 2.3 kV/ cm, and a pump rate of 0.5 mL/hr), with the exception of an extended collection time of 1 hr, while the cylinder angular speed was kept at 69 rpm.

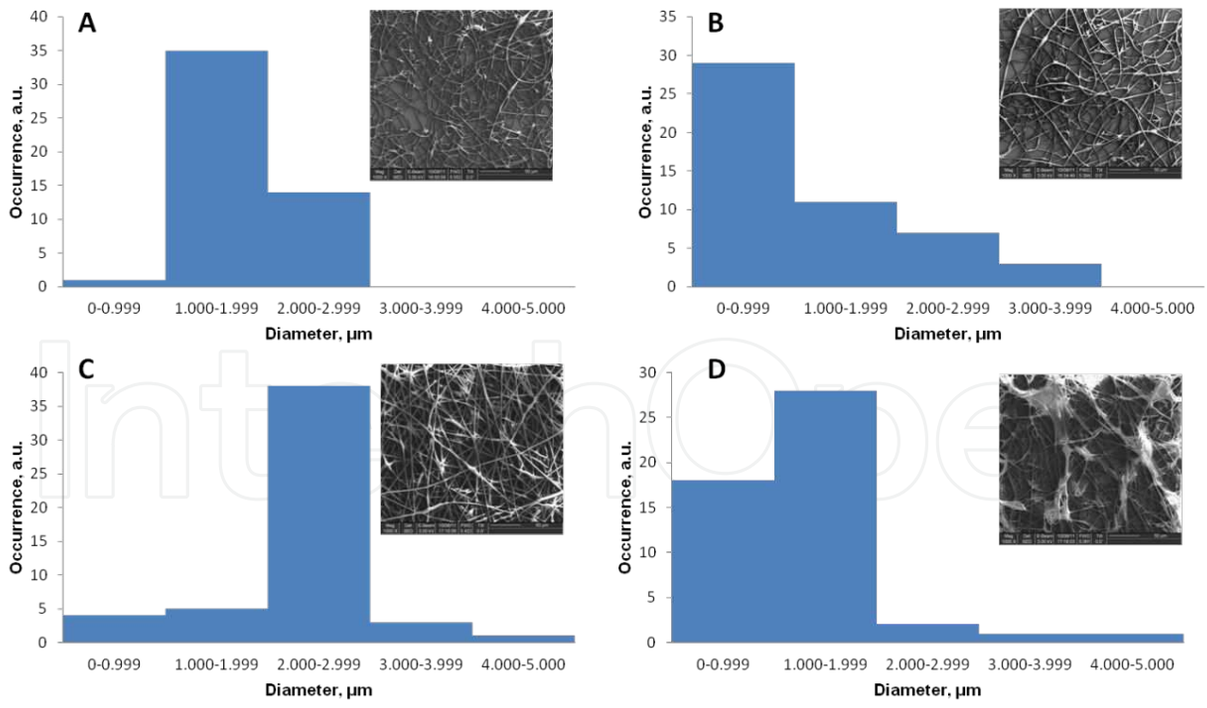

Figure 6. SEM images and histograms for A) 15 % w/v PLLA with 0.2 mg/mL s-MWCNTS B) 15 % w/v PLLA with 1.0 mg/mL s-MWCNTS, C) 15 % w/v PLLA 0.2 mg/mL l-MWCNTS, and D) 15 % w/v PLLA 1.0 mg/mL l-MWCNTS. All in a solution of 1:3 acetone/chloroform.

Other significant characterization techniques, of particular importance in the compositional and structural characterization of carbon allotropes and polymers are infrared (IR) and Raman spectroscopy. In the case of IR spectroscopy (see figure 7), the electric field associated with the photon; excite vibrations of existing dipoles in the material. If the material is crystalline, phonons of differing modes will propagate carrying part of the degenerated energy as heat (motion). In the case of Raman, a laser, with the intense electric field associated to its photons, induce a dipole in the material, and excite dipole oscillations with similar consequences as in IR. Of course, the light emitted by the vibrating charges in both cases (IR and Raman) is used as a signature of the material under study, collected by suitable optics, send to a photo-detector and transduced as a voltage to the processing unit and displayed. Most polymers are IR active, that is, they possess the pertinent dipoles in their structure. For these materials IR spectroscopy is a useful characterization tool, as most spectra are tabulated and indexed. In the case of carbonaceous materials, Raman spectroscopy is the technique of choice, as their spectrum, shows two prominent peaks around 1350 and 1600 cm^{-1}. (see figure 8) The peak at ~ 1350 wave numbers is a disorder induced response, and the other, ~1600 cm^{-1}, is a Raman-allowed mode found in highly oriented pyrolytic graphite (HOPG). The ratio of the intensity of both peaks often correlates with order and crystallinity [17]. In order to have a large SSA material, its crystallinity (order) is compromised and these spectroscopic tools become excellent local structural characterization instruments.

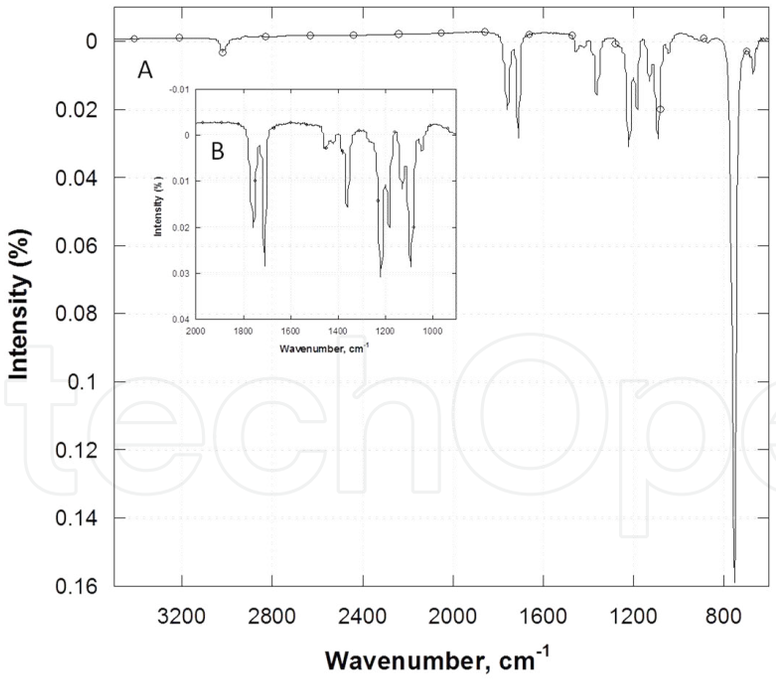

Figure 7. IR spectra for A) PLLA in 1:3 acetone/chloroform B) insert: bands at 1763 cm^{-1} and 1714 cm^{-1} assigned to the ester carbonyl and carboxylic acid carbonyl functional group respectively can be observed together to the OH bend at 1361 cm^{-1} and 1093 cm^{-1}, the C-O stretch can be observed at 1223 cm^{-1}. The strong band at 750 cm^{-1} is due to the S-C stretch because the samples were mounted in silicon wafers.

http://dx.doi.org/10.5772/57094

The interaction between mathematical modeling and experiments often can be mutually beneficial. A theoretical framework can provide experiments with the "backbone" of predictability. Clear correlations by fitting experimental results to a suitable theory helps the scientist decide how and where to do the next experiment, and to "understand" results, errors and fluctuations. The problem is that at times, analytical results are difficult or impossible to obtain. In that case the scientist often utilize numerical methods with the aid of a plethora of commercially available software packages of ease implementation in a personal computer. The software of our choice is COMSOL™. We like this software for its versatility, friendliness, and economy [18]. This software is capable of coupling the PDE's for mechanics, heat, E&M, acoustic, electro-chemistry and others. We have used it for about a decade now, and really benefited from it.

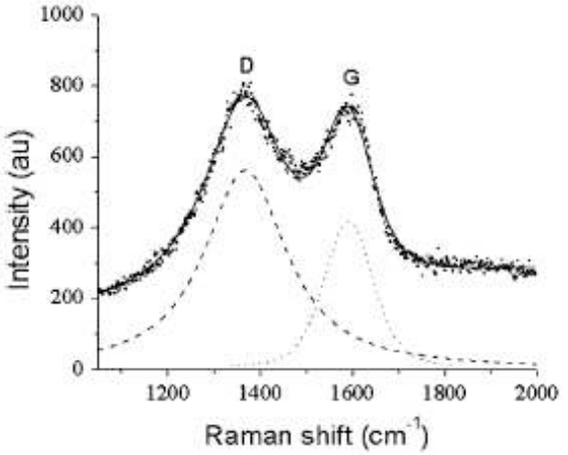

Figure 8. Raman spectrum for a carbonized electro-spun PAN fiber. The first peak, labeled D, correlates with disorder while the second, labeled G correlates with crystallinity.

9. Mechanical properties

The relevance of mechanical properties to the performance of super-capacitors separating membranes stem from the forces and stresses these membranes are exposed during capacitor fabrication, when the material is cut and aligned, as well as during service, when Joule heating generated thermal stresses load the fibers. Since the fibers forming the matt are randomly deposited, they are fluctuating in both on its spatial distributions in the deposition plane, and in fiber diameter. The possibility of having simultaneously a particular spatial location with a particular concentration of small diameter fibers, generating a "soft spot" mechanically and easily deformed by the transported fluid, is finite. Ongoing analytical and simulations research testing this hypothesis is expected to soon yield a predictive model.

The relation between stresses and deformation, at least for small deformations or strain are linear and they have been systematized by solutions to Hookes' Law that, for an anisotropic substance, linearly relates the strain tensor to the stress tensor with the elastic moduli as the

proportionality constant. For a homogeneous isotropic substance, the stress, strain and elastic constants are all scalars with the value of the elastic constants known as the Young's modulus as depicted in equations 5.

$$\sigma_{ij} = c_{ijkl}\varepsilon_{kl} \tag{5}$$

Equations 5, $\sigma_{ij} = c_{ijkl}\varepsilon_{kl}$ (anisotropic media), $\sigma = Y\varepsilon$ (isotropic media), where σ is the symbol for stress, c for elastic constants, Y for Youngs' modulus, and ε for strain.

Sample ID	Thickness, inches	Cross Section Length, inches	Area, inches^2	UTS, PSI	Breaking Point, PSI	Speed, inches/min	Breaking Time, min	Breaking Time, min/inch^2	Young's Modulus, PSI
GoreTex™	0.0011	0.197	0.00022	3508.97	2787.64	0.5	0.84	3818.18	653.73
15% PLA	0.0018	0.236	0.00042	889.37	728.93	0.3	1.56	3714.29	20.07
(1 mg/mL) s-MWCNT	0.0006	0.236	0.00013	1186.90	957.78	0.1	0.74	5692.31	12.27
(1 mg/mL) l-MWCNT	0.0007	0.236	0.00017	1711.86	1482.08	0.3	0.36	2117.65	29.73

Table 2. Mechanical properties of the mats studied.

There are multiple approximate solutions to Hooke's law for different experimental circumstances. Since the thickness of these permeable separating mats is small compared to the diameter when utilized in super-capacitors, they are bona-fide membranes. There are two types of membranes often encountered in practice [19] namely, the thick and thin membranes. The first type received its name when the maximum deflection at its center (in this case of a circular membrane as often used in super-capacitors) under load, w_o is far smaller than the membrane thickness d_m. The membrane is thin when the deflection is larger than the membrane thickness. The approximations are such that a thick membrane maybe treated as thin as the pressure head increases, and so the deflection. The deflection shape for a thick membrane relates to the torques acting along the circumference where the membrane is clamped. The deflection of a circular thick membrane w, with radius of R_m is described by equation 6. The membranes thickness range between 50 and 150 μm, while the estimated deflections are much smaller (nano-metric), so equation 6 for a thick membrane model the behavior of our separating membranes reasonably well.

$$w(r) = w_0\left(1 - \frac{r^2}{R_m{}^2}\right)^2 \tag{6}$$

Various fibers and mats were prepared for mechanical test as well as for morphological analysis. The mechanical strength was measured using the INSTRON (Model 4206), the sample were cut it with "doggy bone" configuration [20]. During the experiment, both ends of the

http://dx.doi.org/10.5772/57094

sample are clamped. The upper end is vertically pulled up at a constant force and velocity, until the samples fracture. From the geometry and strain rate information one can infer the value of the composite Young's modulus. Table 2 summarize the results for mechanical test for mats obtained from the electro-spinning of 15 % w/v PLLA solutions in 1:3 acetone/ chloroform with MWCNTs in comparison with currently use membrane in our laboratory, GoreTex™.

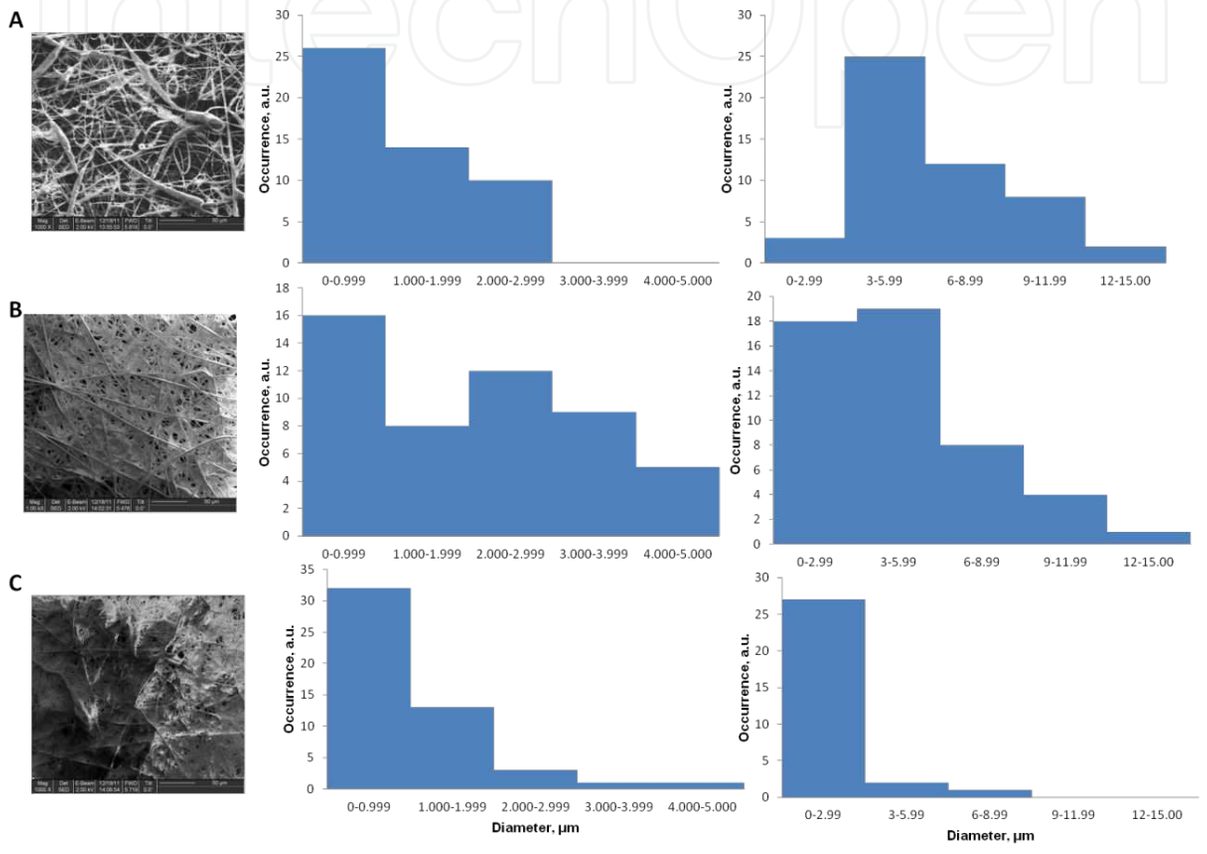

Figure 9. SEM with corresponding histogram analysis for fibers diameter and pores diameter for A) 15 % w/v PLLA B) 15 % w/v PLLA with 1.0 mg/mL s-MWCNTS, C) 15 % w/v PLLA 1.0 mg/mL l-MWCNTS in 1:3 acetone/chloroform.

It can be observed from our results that the Young's modulus decreases from l-MWCNTs (29.73 PSI) > 15 % PLA (20.07 PSI) > s-MWCNTs (12.27 PSI), this can be correlated with the mats fiber diameters distribution, where the number of nanometric diameter fibers increases in the same order: l-MWCNTs > 15 % PLA > s-MWCNTs. However, the number and dimensions of pores, decreases in the following order, 15 % PLA > s-MWCNTs > l-MWCNTs (figure 9). It has been reported previously that the Young's modulus in nonwoven fabrics is affected by porosity, fiber diameter, radius of curvature, and the distance between the junctions where fibers cross [21]. Therefore, not a single factor is responsible for the mechanical properties, but we can see a trend in our results that smaller fiber composition, together with bigger pores seems to somewhat enhance the Young's modulus. In comparison, the GorTex™ membrane has a higher Young's modulus, as it is expected for woven fabrics. We test the performance of the membrane

produced from the 15% w/v PLA solution to that of the GorTex for one of our devices. The decision to use the 15% w/v PLA membrane was done under the bases that this membrane posses more uniformity in the average pores' size than the others.

10. Concluding remarks

The device utilized to test the suitability of the PLLA based composite membrane was a pseudo-capacitor device, using as electrode material the oxidized and neutralized species of poly-3,4-propylenedioxythiophene (the process for the construction of this device have been previously reported by our group) [22,23]. The results indicated (figure 10) that over slow charging-discharging rates our membrane performed better than the bench mark membrane, but as we moved from moderate to fast charge-discharge rates, the performance of both membranes are comparable.

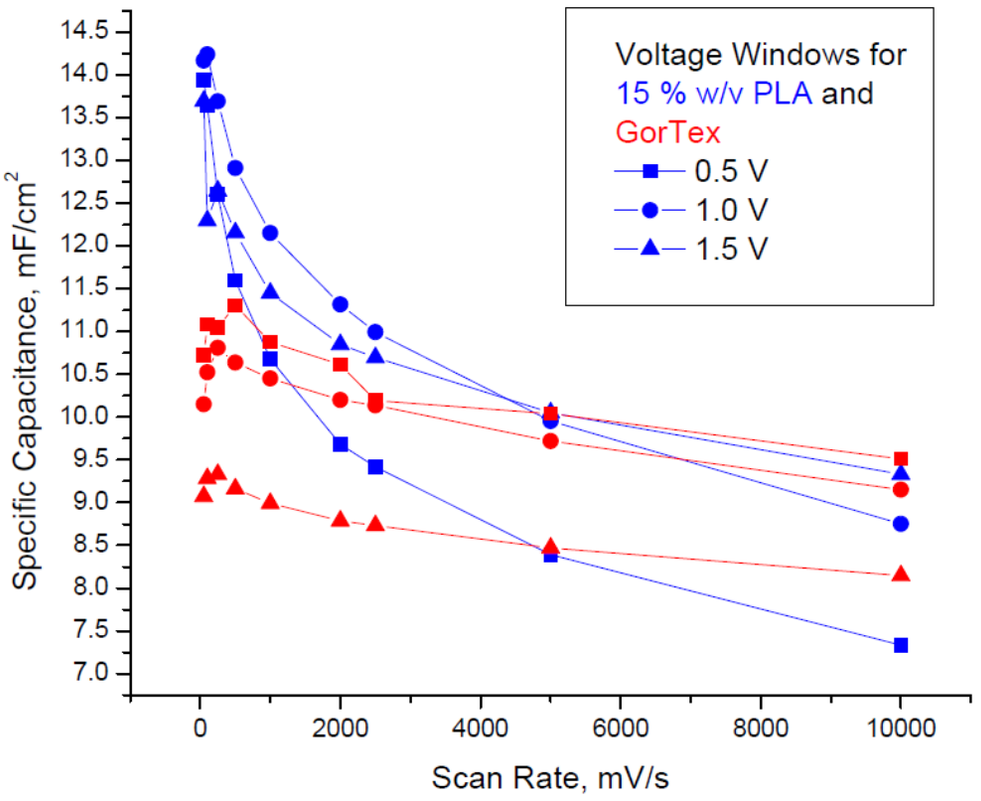

Figure 10. Specific capacitance as a function of scan rate and voltage window for poly-3,4-propylenedioxythiophene pseudo-capacitor using GorTex™ and PLLA separator membranes.

http://dx.doi.org/10.5772/57094

Acknowledgements

We would like to acknowledge support from the following sources:

The Penn's Nano-Bio Interface Center (NBIC) through the NSF sponsored grant NSEC DM R08-32802.

R. Cardona would like to acknowledge the University of Pennsylvania Provost Office and the Laboratory for the Research on the Structure of Matter (LRSM) through the NSF grant DMR11-20901 for her support as a postdoctoral fellow.

We like to acknowledge the SEM microscopy work of our collaborator Prof. Eva Campo from Penn' s LRSM.

We acknowledge the help offered by our graduate students Mr. Timothy Jones, and Hitesh Sahoo, as well as the NSF – REU sponsored undergraduates Mr. Matt Biggers, Mr. Esteban Villareal, Mr. Raymond Xu, Mr. Melvin Berrios and the two H.S. interns, Mr. Adam Flecher and the ACS-Seed fellow, Ms. Rebecca Irizarry.

Author details

Rocío del A. Cardona and Jorge J. Santiago-Avilés*

*Address all correspondence to: santiago@seas.upenn.edu

Electrical and Systems Engineering, University of Pennsylvania, Philadelphia, USA

References

[1] R.Kotz, M.Carlen, *Principles and Applications of Electrochemical Capacitors*, Electrochemica Acta, 2000; 45, 2483-2498

[2] H.D. Abruña, Y.Kiya, J.C.Henderson *Batteries and electrochemical capacitors*. Physics Today. 2008, 43-47

[3] C.A. Vincent, and B. Scrosati. Modern Batteries. In: Butterworth, Oxford; 1997.

[4] B.E. Conway. Electrochemical Supercapacitors. In: Plenum Publishers, N.Y. ;1999.

[5] Yury Gogotsi. Carbon Nanomaterials. In: CRC Press; 2006.

[6] E. P. Moore. Polypropylene Handbook. Polymerization, Characterization, Properties, Processing, Applications. In: Hanser Publishers, N.Y.; 1996.

[7] Gore Text. http://en.wikipedia.org/wiki/Gore-Tex (accessed August 2 2012)

[8] Mauritz, K. A., Moore, R. B. State of Understanding of Nafion. Chemical Reviews 2004; 104 (10) 4535–4585.

[9] Burger, C., Hsiao, B.S., Chu, B. Nano-fibrous Materials and Their Applications. Annual Reviews of Material Research. 2006; 36, 333–368.

[10] Mehta, R., Kumar, V., Bhunia, H., Upadhyay, S.N. Synthesis of Poly(Lactic Acid): A Review. Journal of Macromolecular Science. 2005; 45, 325-349.

[11] Gupta, B., Revagade, N., Hilborn, J. Poly(lactic acid) fiber: An overview. Progress in Polymer Science. 2007; 32, 455-482.

[12] Södergård, A., Stolt, M. Properties of lactic acid based polymers and their correlation with composition. Progress in Polymer Science. 2002; 27 (6), 1123–1163.

[13] Harris, A. M., Lee, E.C. Injection molded Polylactide(PLA) composites for automotive applications. Material Research and Advanced Engineering, Ford Company. http://speautomotive.com/SPEA_CD/SPEA2006/PDF/c/c1.pdf (Accessed August 2 2012).

[14] Rosario-Canales, M., Derias, P., Therien, M.J., Santiago-Aviles, J.J., Composite Electronic Materials Based on Poly(3,4-propylenedioxythiophene) and Highly Charged Poly(aryleneethynylene)-Wrapped Carbon Nanotubes for Supercapacitors, ACS Applied Materials and Interfaces. 2012; 4 (1), 102–109.

[15] Li, D., Xia, Y. Electrospinning of Nanofibers: Reinventing the Wheel?. Advanced Materials. 2004; 16, 1151-1170.

[16] Bal, S., Samal, S.S. Carbon nanotube reinforced polymer composite-A state of the art. Bulletin of Material Science. 2007; 30(4), 379-386.

[17] Fung, A.W.P., Rao, A.M., Kuriyama, K., Dresselhaus, G., Endo, M., Shindo, N. Raman scattering and electrical conductivity of highly disordered activated carbon fibers. Journal of Material Research. 1993; 8 (3), 489-500.

[18] Wang, Y., Ramos, I., Santiago-Aviles, J.J. Nanofibers "Diversity of Nano-fibers from Electro-spinning: from Graphitic Carbons to Ternary Oxides". In: INTECH publishers, Croatia; 2010. P89-120.

[19] Szegö, G. On Membranes and Plates. Proceedings of the Natural Academy of Science of the United States of America. 1950; 36(3), 210–216.

[20] Herrmann, A.M. Instrumentation for multiaxial mechanical testing of inhomogeneous elastic membranes. http://hdl.handle.net/1721.1/35671 (accessed August 2 2012).

[21] Pai, C-L., Boyce, M.C., Rutledge, G.C. On the importance of fiber curvature to the elastic moduli of electrospun nonwoven fiber meshes. Polymer. 2011; 52, 6126-6133.

[22] Rosario-Canales, M., Deria, P., Gopu, P., Therien, M., Santiago-Aviles,J.J. Composite Electronic Materials for Super-capacitor Applications, ECS Transactions. 2009; 23(1), 3-10.

[23] Partial content of this work was presented by the author (R. delA Cardona) at 2nd International Conference on Electrospinning, Jeju, S. Korea, 2012, Poly-l-Lactic Acid Membranes Produced by Electrospinning for Applications in Electrical Double Layer Capacitors.

IntechOpen

IntechOpen